Macromolecular Reaction Engineering
www.mre-journal.de

A Closed-Loop Control Strategy for Producing Nitrile Rubber of Uniform Chemical Composition in a Semibatch Reactor: A Simulation Study

*Luis A. Clementi, Romina B. Suvire, Francisco G. Rossomando, and Jorge R. Vega**

To improve the quality of industrial nitrile rubbers, the copolymer chemical composition, $p_A(t)$, should ideally be kept constant along the reaction. This work proposes a closed-loop control strategy for the semibatch operation of the reactor with the aim of regulating $p_A(t)$ within a reduced range of variability. The proposed strategy is evaluated by simulating a mathematical model of the process. To this effect, a simplified mathematical model of the reaction is first derived and then utilized to obtain a suboptimal control law and a soft-sensor that estimates the polymerization rates. The suboptimal control law is compensated by adding a term proportional to errors in $p_A(t)$. The simulated example considers the production of the low-composition AJLT grade, with the copolymerization reaction represented by a detailed mathematical model adjusted to an industrial plant. Due to the high performance of the soft-sensor, the simulation results suggest that the proposed closed-loop strategy is efficient to adequately regulate $p_A(t)$ in spite of structural and parametric uncertainties, while other quality variables remained practically unaffected.

1. Introduction

Commercial grades of nitrile rubber—also known as nitrile-butadiene rubber (NBR)—are typically obtained in industry through the following steps: (i) the production of a synthetic latex of around 20–25% in solids through an emulsion copolymerization of acrylonitrile (A) and butadiene (B), (ii) the recovery of the unreacted (or residual) monomers to then be used in other batches, (iii) the latex coagulation and dewatering to form a crumb rubber, and (iv) a drying and compression stage to produce NBR bales. In the industry, the copolymerization is typically carried out in a batch reactor at a constant reaction temperature of around 10 °C (cold NBR process). Most quality properties of the NBR can be defined during the copolymerization reaction. Also, according to specifications of commercial NBR grades and desired production levels, the copolymerization processes can either be carried out in a batch or semibatch reactor, or in a train of continuous stirred tank reactors.[1]

Industrial reactors for production of NBR are typically operated in batch. From a process control point of view, the batch operation is simple because only the reaction temperature is regulated to avoid deterioration in the copolymer quality. Alternatively, reagent profiles could be added along the polymerization to improve the quality of the final product. To these effects, numerical simulations of mathematical models of the reaction are useful to evaluate the efficiency of different control policies before their practical implementations in the real plant.

Some variables typically used for the molecular characterization of the A–B copolymer are: the average chemical composition (i.e., the average mass fraction of A bounded to the copolymer, $\overline{p}_A$), the (number- and weight-) average molar masses ($\overline{M}_n$ and $\overline{M}_w$), and the average number of (tri- or tetrafunctional) long-chain branches ($\overline{B}_{N,3}$ and $\overline{B}_{N,4}$). Main quality variables of commercial NBR grades are $\overline{p}_A$ and the Mooney viscosity (MV), which is important variable from the point of view of the rubber processability.[2] The MV is related to the average molar masses, and can indirectly be affected by impurities in the recycled A that reduce the effective initiator amounts.[3]

Particularly, $\overline{p}_A$ is an important quality variable that is sometimes used in commercial specifications of NBR because it strongly affects several final properties of the material, such as the glass-transition temperature (T_g), the resistance to fuels and abrasion, and the gas permeation.[1,4] Moreover, $\overline{p}_A$ can also affects MV.

Some commercial grades of NBR are AJLT, BJLT, and CJLT, which are classified according to their values of $\overline{p}_A$, T_g, and MV.

Dr. L. A. Clementi, Prof. J. R. Vega
INTEC, CONICET and Universidad Nacional del Litoral
Güemes 3450, S3000GLN Santa Fe, Argentina
E-mail: jvega@santafe-conicet.gov.ar
Dr. L. A. Clementi, Prof. J. R. Vega
Facultad Regional Santa Fe
Universidad Tecnológica Nacional
Lavaisse 610, S3004EWB Santa Fe, Argentina
R. B. Suvire
Instituto de Ingeniería Química
Universidad Nacional de San Juan
Av. Libertador San Martín Oeste 1109
5400 San Juan, Argentina
Dr. F. G. Rossomando
Instituto de Automática
CONICET and Universidad Nacional de San Juan
Av. Libertador San Martín Oeste 1109
5400 San Juan, Argentina
The ORCID identification number(s) for the author(s) of this article can be found under https://doi.org/10.1002/mren.201700054.

DOI: 10.1002/mren.201700054

Typical nominal values are: $\overline{p}_A \approx 20\%$, $T_g = -56$ °C, and MV = 40–50, for the AJLT grade; $\overline{p}_A \approx 35\%$, $T_g = -37$ °C, and MV = 40–50, for the BJLT grade; and $\overline{p}_A \approx 38\%$, $T_g = -27$ °C, and MV = 20–30, for the CJLT grade. In general, the copolymer chemical composition computed as the (accumulated) mass fraction of A bounded to the copolymer until time t, $p_A(t)$, varies along the reaction. Consequently, the compositional drift could produce undesired heterogeneous materials that exhibit multiple glass transitions and phase separations.[5–7] Similarly, time evolutions of all quality variables are expected: $M_n(t)$, $M_w(t)$, $B_{N,3}(t)$, and $B_{N,4}(t)$. Note that the average global values of these variables coincide with their values at the final reaction time (t_f), for example, $\overline{p}_A = p_A(t_f)$.

The emulsion copolymerization of A and B is characterized by an azeotropic composition point that is close to 40%. Since grades BJLT and CJLT have nominal specifications of $\overline{p}_A$ relatively close to (but below) the azeotropic composition, then a low compositional drift is expected along the polymerization, and therefore almost uniform products can be obtained through batch processes.[8] By contrast, the grade AJLT ($\overline{p}_A \approx 20\%$) importantly differs from the azeotropic point; and therefore, a batch reaction process will produce a meaningful compositional drift characterized by a decreasing $p_A(t)$ profile. Consequently, a highly heterogeneous final material will be obtained through batch reactions. To avoid a deteriorated polymer quality, the copolymerization reaction is typically stopped at $x < 75\%$. This fact positively contributes to limit the compositional drift that would be more important if higher conversion levels were reached.

Detailed mathematical models of the semibatch copolymerization of A and B have been originally published by Dubé et al.[9] and Vega et al.[10] Even though meaningful differences have been detected in a few parameters of both models,[11] the main simulated variables were checked to exhibit a low sensitivity to such parameters. The model parameters determined by Vega et al.[10] were adjusted to reproduce experimental data collected in an industrial plant. In general, the NBR copolymerization model can be thought as being composed by three modules partially coupled:[12] (1) the mass balance module (MBM), (2) the molar mass module (MMM), and (3) the energy balance module (EBM). At each time, the MBM allows the calculation of the main reaction variables, such as: $p_A(t)$; the accumulated mass conversion, $x(t)$; the volume of each phase, $V_j(t)$ ($j = m$: monomer, w: water, and p: polymer); the monomer concentration in phase j, $[A]_j(t)$ and $[B]_j(t)$; the chain transfer agent (or modifier) concentration in phase j, $[X]_j(t)$; and the A and B polymerization rates, $R_A(t)$ and $R_B(t)$; among other variables. The main MMM outputs are $M_n(t)$, $M_w(t)$, $B_{N,3}(t)$, and $B_{N,4}(t)$. The EBM predicts the reactor temperature, $T(t)$, and the mass flow rate of evaporated refrigerant, $G_R(t)$.

In practice, some process variables of the EBM are easy to be measured online, as for example, $T(t)$ and $G_R(t)$, although unfortunately industrial $G_R(t)$ measurements exhibit meaningful noises.[12] By contrast, most polymerization variables that are included in the MBM and MMM cannot be measured online due to the lack of specific sensors. For the isothermal NBR process, the estimation of $x(t)$ from measurements of $G_R(t)$ is relatively simple.[12] By contrast, the estimation of NBR quality variables is rather difficult. Based on calorimetric measurements, Gugliotta et al.[12] proposed an open-loop observer for the online estimation of several variables in an industrial NBR plant. Such observers were then used to calculate optimal control laws that allowed the regulation along the polymerization of (a) $p_A(t)$, by manipulation of the A feed flow rate, and (b) $M_n(t)$, $M_w(t)$, $B_{N,3}(t)$, and $B_{N,4}(t)$, by manipulation of the X feed flow rate.[13,14] Regarding a practical implementation in industry, the efficiency of those observers could be limited by (i) the unavoidable structural and parametric errors of the mathematical models utilized for their derivations, (ii) the presence of frequent disturbances (e.g., impurities in the reactants, measurement noises, etc.), and (iii) uncertainties in the initial charge recipe.

The production of NBR in a train of eight continuous stirred tank reactors (CSTR) has been investigated on the basis of a mathematical model.[15,16] Steady-state feed flows of A, B, and CTA added into intermediate reactors of the train were calculated to maximize the production of NBR with prespecified values of $\overline{p}_A$ and $\overline{M}_w$.[16] Also, a practical procedure for minimizing the off-spec generated during changes of grade (from AJLT to BJLT, and vice versa) was proposed and successfully evaluated through simulations.[17] Different operation scenarios of a train of eight reactors utilized for the NBR production were discussed by Madhuranthakam and Penlidis.[18] Washington et al.[11] presented a complete mathematical model that is useful to simulate the NBR polymerization in batch or continuous reactors, as well as in a train of CSTRs. Even though a train of CSTR can compensate the compositional drift through proper monomer feeds at intermediate reactors, the regulation of the chemical composition in a semibatch operation is still of interest for current NBR processes of low production scales.

In summary, although several strategies were proposed to produce NBR of predefined quality properties, all quality variable estimators (soft-sensors) as well as the proposed control laws were first derived and then evaluated on the same mathematical model utilized for representing the copolymerization reaction. In general, it is accepted that the implementation of efficient closed-loop control strategies is an unsolved challenge yet due to (i) nonlinearities of the polymerization process, (ii) structural and parametric uncertainties in the utilized mathematical models, (iii) lack of sensors for online measuring the involved variables, (iv) noisy signals produced by the few available sensors, and (v) difficulties inherent to the online estimation of the quality variables to be controlled. As far as the authors are aware, closed-loop control strategies aimed at regulating quality variables of the A–B copolymer under presence of structural and parametric uncertainties have not been investigated yet.

In this work, a closed-loop control strategy for the semibatch operation of the isothermal NBR reactor is proposed with the aim of regulating $p_A(t)$ along the emulsion copolymerization, by manipulation of the inlet flow rate of monomer A. The proposed strategy is evaluated through several simulations. To these effects, the copolymerization reaction is represented through a detailed mathematical model adjusted to an industrial NBR plant.[10] To turn realistic the closed-loop simulations, a simplified mathematical model of the reaction is first derived and then used to obtain: (i) a suboptimal control law that calculates the inlet flow rate of A for regulating $p_A(t)$ at a given desired value; and (ii) a neural network-based soft-sensor for

estimating the state variables of the reaction that are involved in the calculation of the control law. The soft-sensor requires information on the ratio between the moles of A and B initially charged into the reactor, the mass flow rate of A, and the mass flow rate of the evaporated refrigerant; and from those measurements, it estimates the monomer polymerization rates, $R_A(t)$ and $R_B(t)$. From such estimates, the chemical copolymer composition, $p_A(t)$, is calculated. The ultimate control law is obtained by compensating the errors of the suboptimal control law with a term proportional to the instantaneous error in $p_A(t)$. The proposed closed-loop strategy is evaluated by simulating the production of NBR grade AJLT with the copolymer chemical composition regulated at its nominal value of 20%. Alternative scenarios are also considered for checking the robustness under uncertainties.

2. The Proposed Control Law

The basic idea is to find the inlet molar flow of monomer A, $F_{A,in}(t)$, to be fed into the reactor with the aim of regulating $p_A(t)$ at a constant desired value, p_A^d. Appendix A presents a simplified mathematical model of the copolymerization useful for control purposes. It was derived from the detailed mathematical model by Vega et al.[10] The optimal control law based on the simplified model was derived in Appendix B. This control law is suboptimal for the true process due to differences between both models.

The proposed control law is composed by two additive terms. The first term is selected as the suboptimal control law, $F^*_{A,in}(t)$, given by Equation (B7). The second term should be chosen to compensate for the remaining instantaneous error, $p_A^d - p_A(t)$. Unfortunately, in practice the polymerization rates, $R_A(t)$ and $R_B(t)$, involved in Equation (B7), and the chemical composition, $p_A(t)$, cannot be measured online, and therefore their values must be estimated by means of an adequate soft-sensor (see next section). Then, the control law can be implemented as follows

$$F_{A,in}(t) = \left(\hat{R}_A(t) - \frac{\hat{R}_B(t)}{\beta} \right) + K_p \left(p_A^d - \hat{p}_A(t) \right) \quad (1)$$

where the symbol "^" represents the estimated value of a given variable. In Equation (1), K_p is a constant (a proportional gain), p_A^d is the desired value of p_A (or the set-point), $\hat{R}_A(t)$ and $\hat{R}_B(t)$ are the estimated polymerization rates, and $\hat{p}_A$ can be calculated on the basis of $\hat{R}_A(t)$ and $\hat{R}_B(t)$, as follows (see Appendix A)

$$\hat{p}_A = \frac{M_A \hat{N}_{A,b}(t)}{M_A \hat{N}_{A,b}(t) + M_B \hat{N}_{B,b}(t)} = \frac{M_A \int_0^t \hat{R}_A(t)dt}{M_A \int_0^t \hat{R}_A(t)dt + M_B \int_0^t \hat{R}_B(t)dt} \quad (2)$$

where $\hat{N}_{A,b}$ and $\hat{N}_{B,b}$ are the total moles of reacted A and B, and M_A (= 53.06 g mol^{-1}) and M_B (= 54.09 g mol^{-1}) are the molar masses of monomers A and B.

The second term of Equation (1) is proportional to the estimated instantaneous error, $p_A^d - \hat{p}_A(t)$. In this case, a classical integral term in Equation (1) is not recommended to be included because: (i) $p_A(t)$ is an accumulated variable that is obtained by integration of the instantaneous polymerization rates (Equation (2)), and therefore an additional integral term might lead to instabilities, and (ii) typical restrictions on the manipulated variable, $F_A(t)$, such as saturations that avoid negative feed flows, could cause undesired windup effects.

Figure 1 presents a basic scheme of the proposed closed-loop system that also includes the soft-sensor. Additive noises $\Delta G_{A,in}$ and ΔG_R were added to turn more realistic the simulated measurements that are then fed into the soft-sensor.

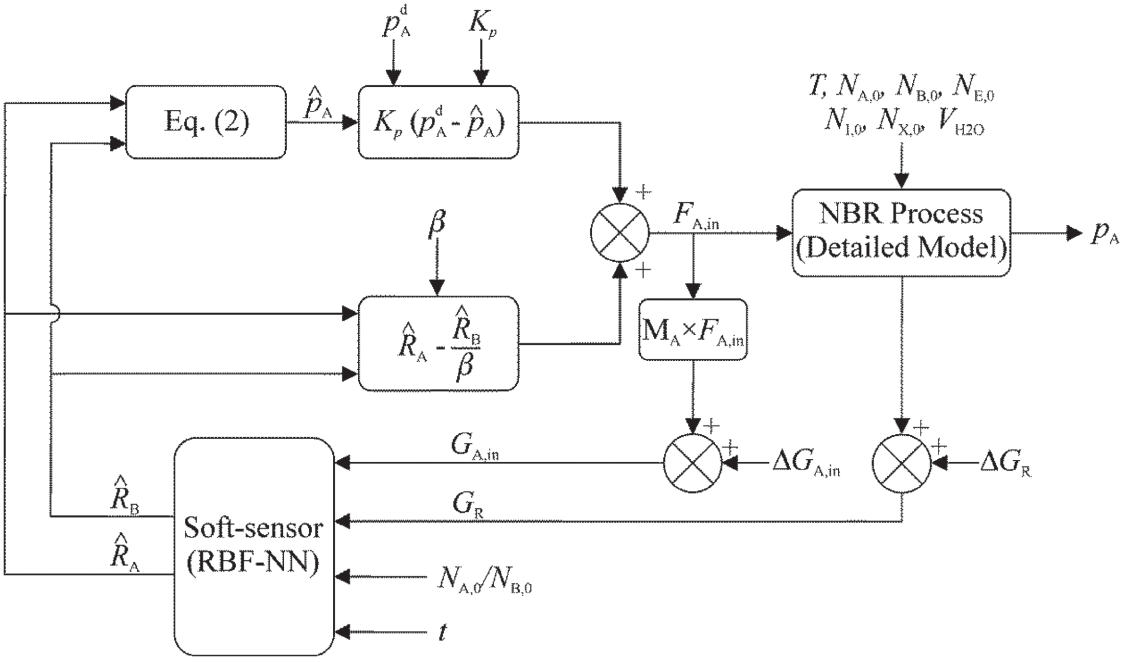

Figure 1. Schematic representation of the closed-loop control strategy for regulating $p_A(t)$ at the desired value, p_A^d.

3. The Proposed Soft-Sensor

A soft-sensor is a model that is used to online estimate non-measurable process variables from the knowledge of other measured process variables. Soft-sensors can be used for monitoring and/or control purposes in complex industrial processes. Artificial neural networks are often utilized to implement soft-sensors due to their ability to efficiently map the highly nonlinear dynamics that are typically present in many industrial processes. In a styrene–butadiene emulsion polymerization system, a neural network proved efficient to estimate both production and quality variables.[19] For the current polymerization process, the soft-sensor of **Figure 2** is proposed for estimating the polymerization rates $R_A(t)$ and $R_B(t)$ involved in Equation (1). For such purposes, a radial basis function neural network (RBF-NN) that includes a single hidden layer of K neurons,[20] is fed with four inputs: (1) the noisy measurements of the accumulated mass flow of the evaporated refrigerant, $G_R^{Acc.}(t) = \int_0^t [G_R(t) + \Delta G_R(t)]\,dt$, (2) the noisy measurements of the accumulated mass flow of A fed into the reactor, $G_{A,in}^{Acc.}(t) = \int_0^t [M_A F_{A,in}(t) + \Delta G_{A,in}(t)]dt$, (3) the ratio between the moles of A and B initially charged into the reactor, $N_{A,0}/N_{B,0}$, and (4) the reaction time, t.

The current choice of an RBF neural network is supported by its universal[20,21] and best approximation[22–24] properties. Besides, an RBF neural network can be used to perform a curve fitting operation in multidimensional spaces; and although it is highly nonlinear in its parameters, its learning procedure has no local minimum problem.[25] This last characteristic represents an evident advantage on other neural network structures such as the multilayer Perceptron that typically exhibits a complex error surface with local minima or nearly flat regions.

At each time t, the RBF-NN receives the input vector $\mathbf{I} = [t, G_R^{Acc.}(t), G_{A,in}^{Acc.}(t), N_{A,0}/N_{B,0}]^T \in \Re^{4\times 1}$; and produces the output vector, $\mathbf{O} = [\hat{R}_A(t), \hat{R}_B(t)]^T \in \Re^{2\times 1}$. The superscript ^{T} indicates transpose vector. The k-th neuron in the hidden layer produces a scalar output of amplitude h_k, given by

$$\xi_k(\mathbf{I}) = \frac{1}{s_k\sqrt{2\pi}} e^{-\frac{\|\mathbf{I}-\mathbf{c}_k\|^2}{2s_k^2}};\ (k = 1,\ldots,K) \tag{3}$$

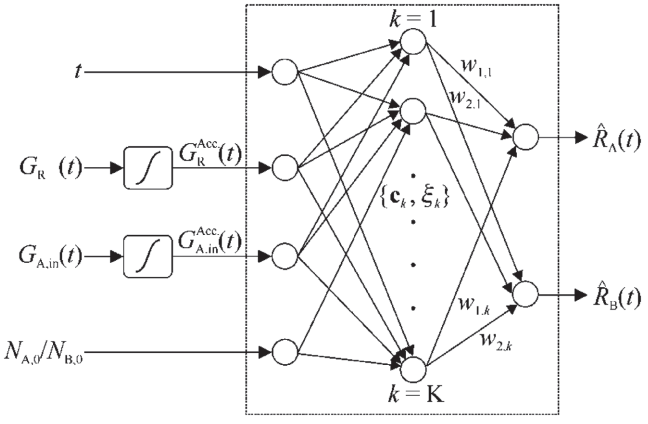

Figure 2. The proposed soft-sensor based on an RBF-NN.

where $\|\mathbf{I} - \mathbf{c}_k\|$ is the Euclidean distance between the input vector $\mathbf{I}$ and the center $\mathbf{c}_k$ (4×1) of the k-th neuron in the hidden layer; and s_k $(k = 1, ..., K)$ is the smoothness parameter that corresponds to the k-th neuron. From $\xi_k(\mathbf{I})$, the output of the RBF-NN is calculated as follows

$$\mathbf{O} = \sum_{k=1}^{K} \xi_k(\mathbf{I})[w_{1,k}\ \ w_{2,k}]^T \tag{4}$$

where $w_{1,k}$, $w_{2,k}$ $(k = 1, ..., K)$ are the weight coefficient of the connection between the k-th hidden neuron and the two output neurons. The center of each hidden neuron, $\mathbf{c}_k$, and the two weights of its connections with the output layer, $\mathbf{w}_k = [w_{1,k}\ \ w_{2,k}]$, are chosen through the training procedure that is described in the following section.

3.1. Training of the RBF-NN

The training procedure of an RBF-NN is fast and simple.[26] In fact, the training patterns are built on the basis of a set of K_t pairs $\{\mathbf{I}_k = [t_k, G_{R_k}^{Acc.}, G_{A,in_k}^{Acc.}, N_{A,0k}/N_{B,0k}]^T \in \Re^{4\times 1}, \mathbf{O}_k = [R_{A_k}, R_{B_k}]^T \in \Re^{2\times 1}\}$ $(k = 1, ..., K_t)$. These patterns are presented to the RBF-NN. A subset with K $(< K_t)$ randomly chosen training patterns is utilized for determining the values of $\mathbf{c}_k$ and $\mathbf{w}_k$ $(k = 1, ..., K)$. Note that the number of hidden neurons, K, coincides with the number of chosen training patterns. The center of the k-th hidden neuron is chosen as $\mathbf{c}_k = \mathbf{I}_k$ $(k = 1, ..., K)$, and the weight coefficients of the connections with the output layer are chosen as $\mathbf{w}_k = \mathbf{O}_k$ $(k = 1, ..., K)$. Consequently, from Equation (4), the RBF-NN produces the following output

$$\mathbf{O} = \sum_{k=1}^{K} \xi_k(\mathbf{I})\,\mathbf{O}_k \tag{5a}$$

with

$$\xi_k(\mathbf{I}) = \frac{1}{s_k\sqrt{2\pi}} e^{-\frac{\|\mathbf{I}-\mathbf{I}_k\|^2}{2s_k^2}};\ (k = 1,\ldots,K) \tag{5b}$$

According to Equations (5a) and (5b), the output of the RBF-NN is obtained as the linear combination of the training patterns $\mathbf{O}_k = [R_A\ R_B]^T$ weighted by the coefficients $\xi_k(\mathbf{I})$ $(k = 1, ..., K)$. Such coefficients become larger when the centers $\mathbf{c}_k = \mathbf{I}_k$ are closer to the input $\mathbf{I}$. Thus, the output of the RBF-NN is mostly defined by those training patterns $\mathbf{O}_k$ that exhibit small distances $\|\mathbf{I} - \mathbf{c}_k\| = \|\mathbf{I} - \mathbf{I}_k\|$.

The smoothness parameters s_k $(k = 1, ..., K)$ affect the selectivity of the hidden neurons. Thus, small s_k values typically increase the selectivity; i.e., only those neurons of small norm $\|\mathbf{I} - \mathbf{I}_k\|$ will meaningfully contribute to the output. On the contrary, high s_k values produce a less selective RBF-NN, and then neurons with larger distances $\|\mathbf{I} - \mathbf{I}_k\|$ will also contribute to the output. Therefore, low values of s_k can lead to rather oscillating profiles for $\hat{R}_A(t)$ and $\hat{R}_B(t)$ around the true profiles. By contrast, high values of s_k will produce smoother estimates but probably with erroneous tendencies. For simplicity, a common smoothness parameter, s^*, is selected for all neurons, which can be chosen according to the Holdout method described by

Park and Sandberg.[27] To this effect, the K* (= K_t – K) patterns that were not used in the selection of $\mathbf{c}_k$ and $\mathbf{w}_k$ are utilized for determining the optimal s^* by solving the following optimization problem

$$\min_{s^*}\left(\sum_{k=1}^{K^*}\left\|\mathbf{O}_k-\hat{\mathbf{O}}_k\right\|\right) \tag{6}$$

where $\hat{\mathbf{O}}_k$ is the estimation of $\mathbf{O}_k$ produced by the RBF-NN. Thus, s^* is the value that best reproduces the K* selected patterns.

4. Simulation Results

The scheme of Figure 1 was implemented for evaluating the closed-loop regulation of $p_A(t)$ along the copolymerization reaction corresponding to the production of NBR grade AJLT, at 10 °C. Although only simulated results are here presented, it is important to highlight that the detailed mathematical model was originally adjusted (for the BJLT grade) to an industrial plant with a stirred-tank reactor of 21 000 dm^3 operated in batch. Currently, the industrial plant is property of Pampa Energía S.A. (San Lorenzo, Santa Fe, Argentina).

The recipe for the batch copolymerization was directly taken from Minari et al.,[15] and it was also used for the semibatch operation, except for a reduction of around 26% in the initial amount of monomer A (see **Table 1**). The true copolymerization reactions were simulated through the complete model by Vega et al.[10] In practice, a perfect mathematical model of the reaction is unavailable. Therefore, in order to better represent a practical case, the simplified mathematical model (see Appendix A) was used for deriving the control law (see Appendix B) and for synthesizing the soft-sensor (see Section 4.2).

Table 1. Recipes for the industrial production of NBR grade AJLT through the batch and semibatch processes.

	Total moles [mol]	Total mass [kg]
Acrylonitrile	Batch: 14 458	Batch: 767
	S. Batch: 10 663	S. Batch: 566
Butadiene	80 366	4347
Water	156 680	8704
Initiator	1.21	0.24
Emulsifier	742.1	214.0
CTA	93.2	18.9

4.1. Batch Simulations

For the batch process, **Figure 3** compares the main output variables obtained from the detailed model by Vega et al.[10] and the simplified model of Appendix A. Simulations were stopped when the copolymer conversion reached $x \approx 72\%$, as a criterion typically used in industrial practice. Parameters of the simplified model were adjusted to reproduce the profiles obtained with the detailed model. Only two parameters of the MBM were adjusted: $r_B = 0.39$ and $K_{Amp} = 2.00$ (their values in the detailed model were 0.30 and 2.20, respectively). To compensate for the average molar masses between both models, the B-transfer propagation constant to CTA, k_{fBX}, was reduced from 241 (in the detailed model) to 201 (in the simplified model). Due to the structural differences between both models, the chemical composition evolutions could not be reproduced perfectly. In fact, some minor differences are observed along the trajectories of the (accumulated) $p_A(t)$ and (instantaneous) $p_{A,i}(t)$ chemical compositions. For example, at the beginning of the reaction (t < 150 min),

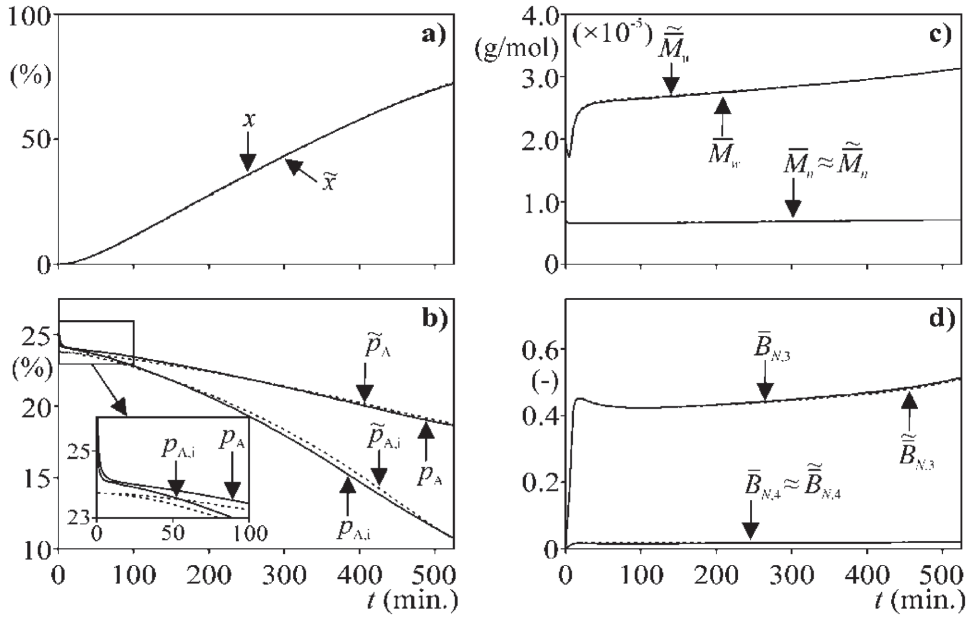

Figure 3. The NBR batch process (AJLT grade): comparison of the detailed (–) and simplified models (- -). a) Mass conversions, b) accumulated and instantaneous chemical compositions, c) number- and weight-average molar masses, and d) tri- and tetrafunctional average long-chain branches. Symbol "~" indicates variables predicted by the simplified model.

differences of ≈0.6% are observed for $p_A(t)$ predicted through both models. At longer times ($t > 400$ min), differences of about 0.2% are observed. However, the other main output variables (x, $\overline{M}_n$, $\overline{M}_w$, $\overline{B}_{N,3}$, and $\overline{B}_{N,4}$) are almost overlapped. The estimated conversion is almost accurate (Figure 3a) because the extent of the polymerization reaction can efficiently be estimated from the measured evaporated refrigerant.[12] Also, the estimated molar masses (Figure 3c) and long-chain branches (Figure 3d) are quite accurate, because highly similar MMM models were used for both the process and the soft-sensor.

Main mismatches between both models are particularly notorious at the first minutes of the reaction. In fact, according to Figure 3b, the detailed model predicted $p_A \approx 1$ for $t \approx 0$, while the simplified model predicted p_A values close to 0.24. It is expected that predictions of the detailed model are more reliable. In fact, at low reaction times, the polymerization of A in aqueous phase leads to the production of poly(acrylonitrile), due to the relatively high solubility of A (and low solubility of B) in water. By contrast, the simplified model considers a negligible concentration of A in water phase (see Appendix A), thus producing lower p_A values at the beginning of the reaction (Figure 3b).

It is important to note the unacceptable compositional drift suffered by $p_A(t)$, which approximately varies from 24% to 18% along the reaction. In practice, such compositional drift can cause an unacceptable heterogeneity in the produced rubber. This is the main reason to implement a control strategy that allows the regulation of the chemical composition along the polymerization reaction.

4.2. Synthesis of the Soft-Sensor

To synthesize the soft-sensor, an RBF-NN with K = 10 000 neurons was selected. The training was carried out through a set of K_t = 10 395 patterns that were generated as follows: (1) the closed-loop of **Figure 4** was implemented; (ii) the simulated copolymerization was carried out for different values of $N_{A,0}$, $N_{B,0}$, K_p, and T, in order to generate the K_t = 10 395 pairs $\{\mathbf{I}_k = [t_k\ G_{R_k}\ G_{A,in_k}\ N_{A,0_k}/N_{B,0_k}]^T,\ \mathbf{O}_k = [R_{A_k}\ R_{B_k}]^T\}$. For such purpose, $N_{A,0}$ was varied from 7500 to 12 500 mol, at regular intervals of 2500 mol; $N_{B,0}$ was varied from 75 000 to 85 000 mol, at regular intervals of 5000 mol; K_p was varied from 0 to 7500, at regular intervals of 750; and T was varied from 9 to 13 °C, at regular intervals of 1 °C. Values of G_R, $G_{A,in}$, R_A, and R_B were taken in the range 1–601 min, at regular intervals of 30 min. Then, K = 10 000 patterns were used for training the RBF-NN, and the remaining K* = 395 patterns were utilized for the selection of the smoothness parameter s^* through the Holdout method, yielding $s^* = 0.95$.

It is worthwhile to mention that the input t_k was proven to play a key role in the performance of the soft-sensor. Evaluations of a soft-sensor synthesized without considering the input t_k produced highly oscillatory and erratic predictions of both polymerization rates. This can be attributed to the rather constant values adopted by R_A and R_B along a period between 100 and 400 min, which could in turn contribute to deteriorate the selectivity of the neural network.

4.3. Semibatch Operation: Closed-Loop Regulation of the Chemical Composition

The main objective of the semibatch operation consists in regulating $p_A(t)$ at the prespecified desired value (p_A^d = 20%) through an appropriate addition of A. The new amount of moles of A to be initially charged into the reactor were calculated through $N_{A,0} = N_{B,0}/\beta$ (see Appendix B), with $\beta = 7.537$ (Equation (B4); while other recipe components were kept unchanged with respect to the batch operation. The proportional constant K_p = 2500 was selected by taken into account that smaller K_p values produced too small contributions of the second term of Equation (1), and consequently more deteriorated regulations of $p_A(t)$. By contrast, higher K_p values produced large oscillations in $G_{A,in}(t)$. Measurements $G_{A,in}(t)$ and $G_R(t)$ were obtained by adding Gaussian noises of zero-mean and standard deviations of 2.5% of the maxima of their noise-free signals. All simulations were stopped when $x \approx 72\%$ was reached, which corresponds to a total reaction time of 522 min.

Figure 5 shows the results corresponding to the proposed semibatch policy. The control strategy produced the A flow rate of Figure 5a, which was able to keep almost constant profiles of both $p_A(t)$ and $p_{A,i}(t)$ around p_A^d = 20% (Figure 5b). Particularly note the meaningful improvement with respect to the batch profiles of Figure 3b, and reproduced as $p_{A,batch}(t)$ and

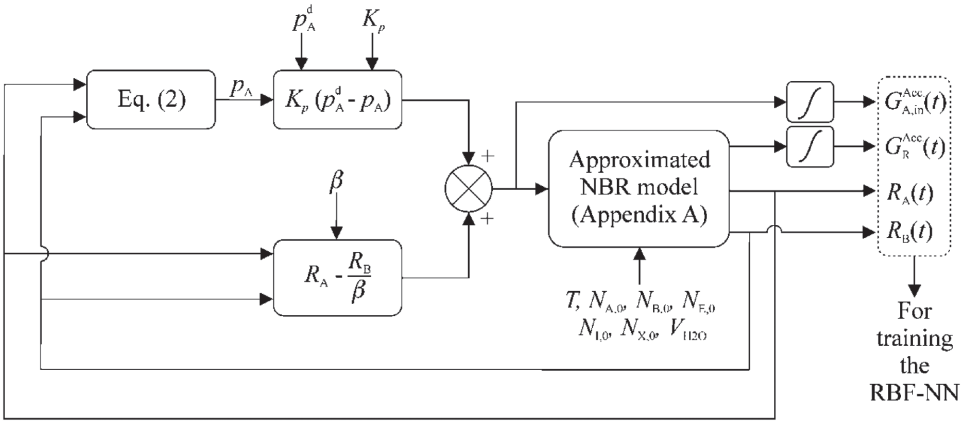

Figure 4. Synthesis of the soft-sensor: closed-loop strategy implemented for generating the training patterns.

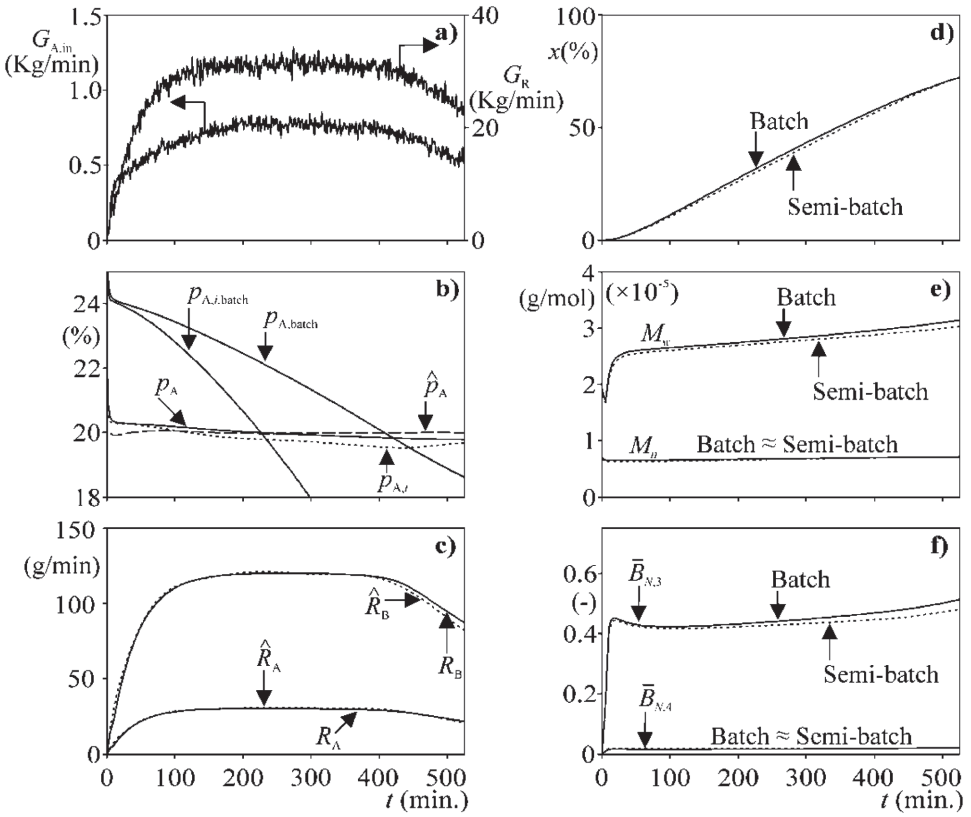

Figure 5. The NBR semibatch process (AJLT grade) and comparison with the batch process. a) Mass feed flow of added A ($G_{A,in}$), and measured mass flow of evaporated refrigerant (G_R), b) accumulated (p_A), instantaneous ($p_{A,i}$), and estimated ($\hat{p}_A$) chemical compositions, c) true (R_A, R_B) and estimated ($\hat{R}_A$, $\hat{R}_B$) polymerization rates, d) mass conversion (x), e) average molar masses ($\bar{M}_n$, $\bar{M}_w$), and f) average degrees of branching ($\bar{B}_{N,3}$, $\bar{B}_{N,4}$).

$p_{A,i,batch}(t)$ in Figure 5b. In general, it was possible to keep $p_A(t)$ within ±0.5% of p_A^d along the reaction, except for the first reaction minutes when the homopolymerization of A in the aqueous phase is dominant. However, the mass of poly(acrylonitrile) produced is almost negligible in comparison to the total copolymer mass. It is also interesting to note that the manipulated flow rate of A, $G_{A,in}(t)$, exhibits a profile almost proportional to the measured mass flow of refrigerant, $G_R(t)$. The total mass of A added along the reaction was 369 kg, as obtained by integration of $G_{A,in}(t)$ of Figure 5a. Then, in the semibatch process the total amount of A was 566 + 369 = 935 kg, which is greater than the 766 kg utilized in the batch process. However, this is an expected result because the final chemical composition (18.6%) reached in the batch process was smaller than the nominal value (20.0%) reached through the semibatch operation.

On the other hand, the mass conversion, x, and the remaining quality variables, $\bar{M}_n$, $\bar{M}_w$, $\bar{B}_{N,3}$, and $\bar{B}_{N,4}$, were almost unaffected by the semibatch policy with respect to the batch reaction (Figure 5d–f). Figure 5c suggests an acceptable performance of the soft-sensor, with estimated polymerization rates close to their true values. For this reason, the estimated chemical composition calculated through Equation (2), $\hat{p}_A(t)$, was close to the true composition, $p_A(t)$ (Figure 5b). In fact, the maximum error reached was 0.4% (except at the beginning of the reaction, due to the homopolymerization of A in aqueous phase).

Even though the calculation $N_{A,0} = N_{B,0}/\beta$ was derived from an approximated model, it was effective to regulate the chemical composition around its desired value. In order to analyze the robustness of the closed-loop strategy under errors in the initial charge of A, three simulations at different initial charges of A were implemented: (i) $N_{A,0} = 0.90 \times N_{B,0}/\beta$, (ii) $N_{A,0} = N_{B,0}/\beta$, and (iii) $N_{A,0} = 1.10 \times N_{B,0}/\beta$. The results are presented in **Figure 6**. In each of the three analyzed cases, $\hat{p}_A(t)$ was close to $p_A(t)$, thus confirming an acceptable performance of the implemented soft-sensor. Note that in case (iii), $p_A(t)$ is quite larger than p_A^d along the first minutes of the reaction. Unfortunately, this error cannot be corrected because the control system is incapable of withdrawing A from the reactor. In this sense, the current simulations show that too low initial charges of A into the reactor can adequately be compensated by the added A flow rate; while excessive amounts of A should be avoided in the initial charge.

A simulation was carried out at $T = 12$ °C, in order to investigate the robustness of the closed-loop strategy under uncertainties in the reaction temperature. **Figure 7** shows some variables of interest. At the selected higher temperature, the propagation constants increased, and therefore the mass conversion reached 72% in a reaction time shorter than in the case of $T = 10$ °C (Figure 7a). Even though the soft-sensor did not include the temperature as an input, the estimated chemical composition profile was acceptably close to the true one. This is an important result because it suggests that $p_A(t)$ can be efficiently controlled through the proposed strategy even under presence of undesired changes or errors in the reaction temperature.

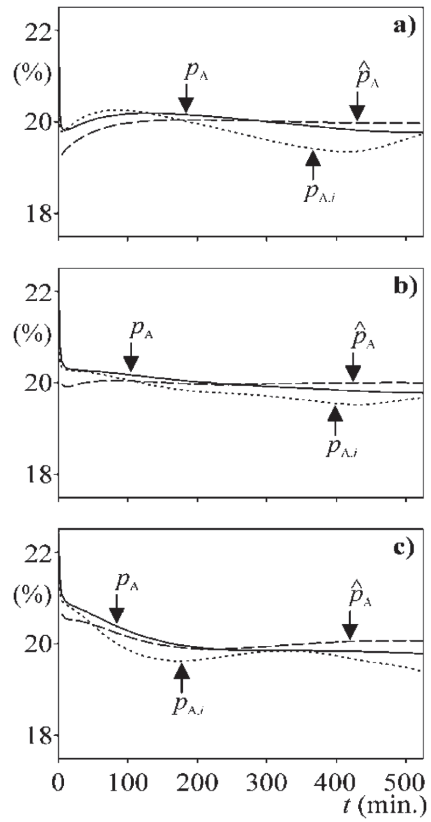

Figure 6. Semibatch NBR operation: sensitivity of the chemical composition to errors in the initial charge of A ($N_{A,0}$). a) $N_{A,0} = 0.90 \times N_{B,0}/\beta$, b) $N_{A,0} = N_{B,0}/\beta$, and c) $N_{A,0} = 1.10 \times N_{B,0}/\beta$.

Other simulations aimed at evaluating the limiting case of Equation (1) when only the suboptimal control law is maintained (i.e., when $K_p = 0$). In this case, reasonable regulations of $p_A(t)$ are obtained provided that accurate $N_{A,0}$ are selected. However, errors in $N_{A,0}$ produced unacceptable off-sets with respect to the desired chemical composition. On the other hand, when only the proportional control law is considered, then the dynamic response of $p_A(t)$ can be poor (for relatively low K_p), or highly oscillatory feed flows of A are obtained even with excessively large peaks. In summary, the combination of both components proposed by Equation (1) seems to be a reasonable solution.

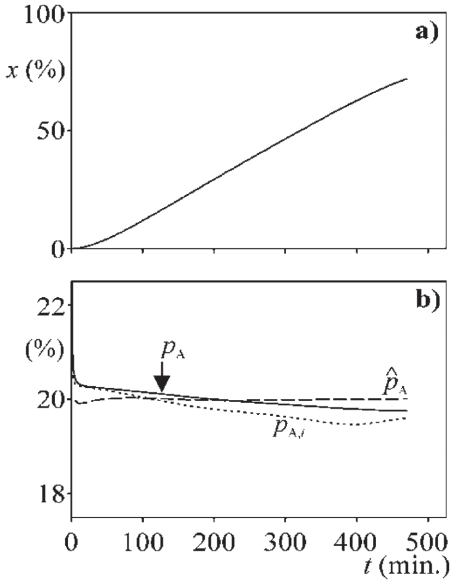

Figure 7. Semibatch NBR operation: sensitivity of the chemical composition to errors in the reaction temperature ($T = 12$ °C). a) Mass conversion, and b) chemical composition profiles.

5. Conclusions

A closed-loop control strategy was proposed and implemented for regulating the chemical composition of the copolymer corresponding to the NBR grade AJLT. A simplified mathematical model of the process was derived, and then used for synthesizing a soft-sensor and for obtaining the control law. The implemented methodology allows for checking the robustness of the proposal, in the sense that the simplified model includes meaningful structural and parametric uncertainties while the real plant was simulated through a detailed mathematical model. Simulation results indicated that the chemical composition can acceptably be regulated along the reaction. With the implemented control scheme, a total compositional drift smaller than 0.5% was obtained, thus importantly reducing the compositional drift of 6% observed in the batch process, and therefore contributing to improve the quality of the final rubber.

Two relevant aspects provide additional reliability to the current closed-loop control strategy: (a) its ability for acceptably compensating errors in the initial charge of A; and (b) its relative insensitivity to errors in the reaction temperature.

Effectiveness of the proposed control law mainly relies on the ability of the soft-sensor for adequately estimating the two reaction rates, R_A and R_B. These estimates have two important roles: (1) they are directly involved in the suboptimal control law; and (2) they are used to estimate the copolymer chemical composition that is then used to compensate for the off-set through the proportional control term. In this context, and regarding to a practical implementation, the correct calibration of the soft-sensor seems to be a crucial stage to obtain an efficient closed-loop strategy.

A negligible sensitivity of the soft-sensor performance was observed when zero-mean random Gaussian noises were added to the variables $G_R(t)$ and $G_{A,in}(t)$. This is due to the filtering effect of the integrations utilized for obtaining the accumulated flows, $G_R^{Acc.}(t)$ and $G_{A,in}^{Acc.}(t)$. Even though not shown, random Gaussian noises with average values larger than 5% with respect to the maximum of $G_R(t)$ and $G_{A,in}(t)$ may deteriorate the soft-sensor performance. These results alert on the importance of a reliable calibration of the corresponding flow meters.

Even though this article only presents simulation results, the industrial implementation of the proposed closed-loop strategy would be simple. Only online measurements of the refrigerant flow are required. The remaining information that is needed as input to the controller (initial monomer loads and reaction time) does not represent major difficulties; while the information on the A feed flow is directly available since it is calculated by the same controller. On the other hand, the training of the neural network (here developed only on the basis of

simulations) could be reinforced by incorporating true measurements taken along the semibatch operations.

Appendix

A. Semibatch Emulsion Copolymerization of A and B: Simplified Mathematical Model of the Mass Balance Module

In this appendix, a simplified mathematical model of the semibatch emulsion copolymerization of A and B is derived on the basis of the detailed mathematical model developed by Vega et al.[10] Most simplifications are introduced in the MBM, and more precisely in the mass balances of the (free and bounded) number of moles of A and B. By contrast, both EBM and MMM are kept unchanged with respect to the original detailed mathematical model.

From Vega et al.,[10] the simplified model is obtained by assuming the following additional hypothesis: (i) the concentrations of A and B in the aqueous phase are negligible in comparison with their concentrations in the polymer phase; and (ii) the partition coefficients of A and B between the monomer and the polymer phases, K_{Amp} and K_{Bmp}, are identical, i.e., $K_{Amp} = K_{Bmp} = K_{mp}$. From hypothesis (i), one can neglect the polymerization rates of A and B in the aqueous phase, i.e., $R_{A,w} = R_{B,w} = 0$. On the other hand, hypothesis (ii) leads to: $[A]_p/[B]_p = N_A/N_B$; i.e., the emulsion copolymerization behaves as a solution copolymerization system. Therefore, under these hypotheses, the mass balance of the free and bounded number of moles of A and B are

$$\frac{dN_A}{dt} = F_{A,in} - R_A \tag{A1}$$

$$\frac{dN_B}{dt} = F_{B,in} - R_B \tag{A2}$$

$$\frac{dN_{A,b}}{dt} = R_A \tag{A3}$$

$$\frac{dN_{B,b}}{dt} = R_B \tag{A4}$$

with

$$R_A = \frac{k_{pAA}\,k_{pBB}\,(r_A[A]_p^2 + [A]_p[B]_p)}{k_{pBB}\,r_A[A]_p + k_{pAA}\,r_B[B]_p}\,\overline{n}\,\frac{N_p}{N_{AV}} \tag{A5}$$

$$R_B = \frac{k_{pAA}\,k_{pBB}\,(r_B[B]_p^2 + [A]_p[B]_p)}{k_{pBB}\,r_A[A]_p + k_{pAA}\,r_B[B]_p}\,\overline{n}\,\frac{N_p}{N_{AV}} \tag{A6}$$

$$[A]_p = \frac{N_A}{K_{mp}V_m + V_p} \tag{A7}$$

$$[B]_p = \frac{N_B}{K_{mp}V_m + V_p} \tag{A8}$$

$$V_p = \frac{M_A N_{A,b} + M_B N_{B,b}}{\rho_p \Phi_p} \tag{A9}$$

$$V_m = \frac{M_A}{\rho_A}N_A + \frac{M_B}{\rho_B}N_B - (1-\Phi_p)V_p \tag{A10}$$

where $F_{A,in}$ and $F_{B,in}$ are the inlet molar feed flows of A and B, respectively; N_A and N_B are the free (or unreacted) moles of A and B; $N_{A,b}$ and $N_{B,b}$ are the moles of A and B bounded to the copolymer; R_A and R_B are the polymerization rates of A and B in the polymer phase; $[A]_p$ and $[B]_p$ are the concentration of A and B in the polymer phase; $\overline{n}$ is the average number of free radicals per polymer particle; N_p is the number of polymer particles; N_{AV} is the Avogadro's constant; k_{pAA} and k_{pBB} are homopropagation rate constants for A and B in the polymer phase; r_A and r_B are the reactivity ratios of A and B; K_{mp} is the (assumed equal) partition coefficient of A and B between the monomer and the polymer phases; V_m and V_p are the volumes of the monomer and polymer phases, respectively; ρ_A, ρ_B, and ρ_p are the densities of the A, B, and the polymer, respectively; and Φ_p is the polymer volume fraction in the polymer phase. From hypothesis (ii), it is also possible to derive the following relationship: $\Phi_p = 1–1/K_{mp}$. For the calculation of $\overline{n}$ and N_p, see, e.g., Vega et al.[10]

After solving the simplified mathematical model of Equations (A1)–(A10), then the main output variables corresponding to the MBM, i.e., the mass conversion, x, and the instantaneous and accumulated mass fractions of A bounded to the copolymer (or instantaneous and accumulated copolymer chemical compositions), $p_{A,i}$ and p_A, can be calculated as follows

$$x(t) = \frac{M_A N_{A,b}(t) + M_B N_{B,b}(t)}{M_A[N_A(t) + N_{A,b}(t)] + M_B[N_B(t) + N_{B,b}(t)]} \tag{A11}$$

$$p_{A,i}(t) = \frac{M_A R_A(t)}{M_A R_A(t) + M_B R_B(t)} \tag{A12}$$

$$p_A(t) = \frac{M_A N_{A,b}(t)}{M_A N_{A,b}(t) + M_B N_{B,b}(t)} \tag{A13}$$

Note that Equations (A11)–(A13) are strictly valid for the simplified model. In the case of the detailed model, $N_{A,b}$ not only includes the moles of A bounded to the copolymer but also the moles of A that homopolymerize in water. Similarly, in the detailed model, R_A also includes the contribution of the A polymerization rate in the water phase.

B. Derivation of the Suboptimal Control Law

Consider the mathematical model of Appendix A. If the instantaneous chemical composition is kept constant along the process, i.e., $p_{A,i}(t) = p_A^d$ (= constant), then Equation (A12) yields

$$p_{A,i}(t) = p_A^d = \frac{M_A R_A(t)}{M_A R_A(t) + M_B R_B(t)} = \frac{1}{1 + \frac{M_B}{M_A}\left(\frac{R_B(t)}{R_A(t)}\right)} \tag{B1}$$

And solving for $R_B(t)/R_A(t)$, it results

$$\left(\frac{R_B(t)}{R_A(t)}\right) = \frac{M_A}{M_B}\left(\frac{1}{p_A^d} - 1\right) = \gamma \tag{B2}$$

where γ is a constant that depends on the chosen p_A^d value. For example, for the AJLT grade ($p_A^d = 0.20$): $\gamma = 3.92$. Since $[A]_p/[B]_p = N_A/N_B$ (see Appendix A), then after replacing Equations (A5) and (A6) into Equation (B2), one obtains

$$\left(\frac{R_B(t)}{R_A(t)}\right) = \frac{r_B\, N_B(t)^2 + N_A(t)\, N_B(t)}{r_A\, N_A(t)^2 + N_A(t)\, N_B(t)} = \gamma \tag{B3}$$

Then,

$$r_B\, \beta^2 - (\gamma - 1)\, \beta - \gamma\, r_A = 0 \tag{B4}$$

where $\beta = N_B(t)/N_A(t)$. Since r_A and γ are constants, then β must be a constant. Therefore, $d\beta/dt = 0$, and one can write

$$N_B(t)\frac{dN_A(t)}{dt} = N_A(t)\frac{dN_B(t)}{dt} \tag{B5}$$

From Equations (A1),(A2), and (B5), it is obtained

$$[F_{A,in}(t) - R_A(t)]\, N_B(t) - N_A(t)\, [F_{B,in}(t) - R_B(t)] = 0 \tag{B6}$$

By assuming $F_{B,in} = 0$, the final expression of the control law is given by

$$F^*_{A,in}(t) = R_A(t) - \frac{R_B(t)}{\beta} \tag{B7}$$

where β is the (positive) solution of Equation (B4) for given values of r_A, r_B, and γ. Equation (B7) is a suboptimal control law in the sense that it was derived from a simplified mathematical model. Additionally, the implementation of Equation (B7) requires the online values of $R_A(t)$ and $R_B(t)$, which cannot be directly measured. In practice, a soft-sensor must be developed to estimate both variables.

Note that the expression $\beta = N_B(t)/N_A(t)$ can also be utilized for the selection of the initial charge of each monomer in the reactor. For example, given an initial amount of B, $N_{B,0}$, then the initial amount of A is $N_{A,0} = N_{B,0}/\beta$.

Acknowledgements

The authors are grateful for the financial support received from CONICET, MinCyT, Universidad Nacional del Litoral, Universidad Tecnológica Nacional, and Universidad Nacional de San Juan.

Conflict of Interest

The authors declare no conflict of interest.

Keywords

acrylonitrile–butadiene rubber, closed-loop control, NBR, semibatch process

Received: October 14, 2017
Revised: December 9, 2017
Published online:

[1] R. E. Kirk, D. F. Othmer, *Encyclopedia of Chemical Technology*, 4th ed., Wiley, New York **1998**.
[2] O. Kensuke, H. Tsutomu, M. Mitsuru, T. Tooru, F. Mitsutoshi, B. Nobuyuki, *Japan Patent, JP52145080*, **1977**.
[3] A. Scott, A. Penlidis, *J. Macromol. Sci., Part A: Pure Appl. Chem.* **2013**, *50*, 803.
[4] D. C. Blackley, in *Emulsion Polymerization and Emulsion Polymers* (Eds: P. Lovell, M. El-Aasser), Wiley, New York **1997**.
[5] A. Guyot, J. Guillot, C. Craillat, M. Llauro, *J. Macromol. Sci., Chem.* **1984**, *A21*, 683.
[6] J. Guillot, in *Polymer Latexes: Preparation, Characterization and Applications, 1st ed., ACS Symposium Series*, Vol. *492* (Eds: E. S. Daniels, E. D. Sudol, M. S. El-Aasser), American Chemical Society, Washington DC **1992**.
[7] P. Canu, S. Canegallo, M. Morbidelli, G. Storti, *J. Appl. Polym. Sci.* **1994**, *54*, 1899.
[8] M. Ambler, *J. Polym. Sci.: Polym. Chem.* **1973**, *11*, 1505.
[9] M. Dubé, A. Penlidis, R. Mutha, W. Cluett, *Ind. Eng. Chem. Res.* **1996**, *35*, 4434.
[10] J. Vega, L. Gugliotta, R. Bielsa, M. Brandolini, G. Meira, *Ind. Eng. Chem. Res.* **1997**, *36*, 1238.
[11] I. Washington, T. Duever, A. Penlidis, *J. Macromol. Sci., Part A: Pure Appl. Chem.* **2010**, *47*, 747.
[12] L. Gugliotta, J. Vega, C. Antonione, G. Meira, *Polym. React. Eng.* **1999**, *7*, 531.
[13] J. Vega, L. Gugliotta, G. Meira, *Polym. React. Eng.* **2002**, *10*, 59.
[14] J. Vega, L. Gugliotta, G. Meira, *Lat. Am. Appl. Res.* **2003**, *33*, 115.
[15] R. Minari, L. Gugliotta, J. Vega, G. Meira, *Lat. Am. Appl. Res.* **2006**, *36*, 301.
[16] R. Minari, L. Gugliotta, J. Vega, G. Meira, *Comput. Chem. Eng.* **2007**, *31*, 1073.
[17] R. Minari, L. Gugliotta, J. Vega, G. Meira, *Ind. Eng. Chem. Res.* **2007**, *46*, 7677.
[18] C. Madhuranthakam, A. Penlidis, *Polym. Eng. Sci.* **2012**, *53*, 9.
[19] R. Minari, G. Stegmayer, L. Gugliotta, O. Chiotti, J. Vega, *Macromol. React. Eng.* **2007**, *1*, 405.
[20] S. Haykin, *Neural Networks: A Comprehensive Foundation*, Prentice Hall, NJ **1999**.
[21] J. Park, I. Sandberg, *Neural Networks* **1993**, *3*, 246.
[22] F. Girosi, T. Poggio, *Biol. Cybern.* **1990**, *63*, 169.
[23] J. Wray, G. Green, *Neural Networks* **1995**, *8*, 31.
[24] P. Yee, S. Haykin, *Regularized Radial Basis Function Networks: Theory and Applications*, John Wiley & Sons, New York **2001**.
[25] M. Bianchini, P. Frasconi, M. Gori, *IEEE Trans. Neural Networks* **1995**, *6*, 749.
[26] L. Jinkun, *Radial Basis Function (RBF) Neural Network Control for Mechanical Systems*, Springer, New York **2013**.
[27] J. Park, I. Sandberg, *Neural Comput.* **1991**, *3*, 246.